AMRA TR 67-03

TEMPERED MARTENSITE EMBRITTLEMENT AND FRACTURE TOUGHNESS IN 4340 STEEL

TECHNICAL REPORT

by

ERIC B. KULA

and

ALBERT A. ANCTIL

JANUARY 1967

U. S. ARMY MATERIALS RESEARCH AGENCY
WATERTOWN, MASSACHUSETTS 02172

F 29

651066

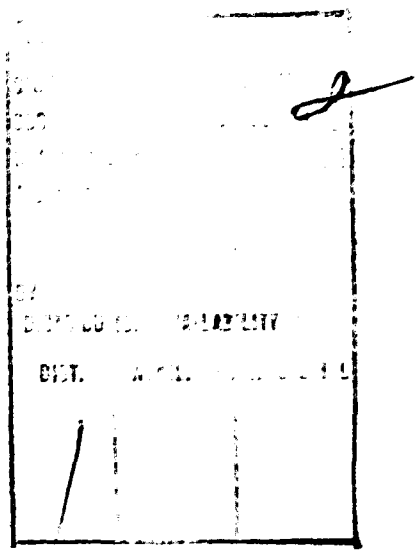

Mention of any trade names or manufacturers in this report shall not be construed as advertising nor as an official indorsement or approval of such products or companies by the United States Government.

The findings in this report are not to be construed as an official Department of the Army position, unless so designated by other authorized documents.

DISPOSITION INSTRUCTIONS

Destroy this report when it is no longer needed.
Do not return it to the originator.

TEMPERED MARTENSITE EMBRITTLEMENT AND FRACTURE TOUGHNESS IN 4340 STEEL

Technical Report AMRA TR 67-03

by

Eric B. Kula

and

Albert A. Anctil

January 1967

D/A Project 1C024401A328

AMCMS Code 5025.11.294

Metals Research for Army Materiel

Subtask 35457

U. S. ARMY MATERIALS RESEARCH AGENCY
WATERTOWN, MASSACHUSETTS 02172

U. S. ARMY MATERIALS RESEARCH AGENCY

TEMPERED MARTENSITE EMBRITTLEMENT AND FRACTURE TOUGHNESS IN 4340 STEEL

ABSTRACT

Tempered martensite embrittlement (500 F embrittlement) has been studied in 4340 steel by means of Charpy impact, tension, and fracture toughness tests carried out over a range of test temperatures. Embrittlement was shown in the impact tests by a minimum in room temperature impact properties for tempering temperatures ranging from 500 to 650 F, the same range for which the transition temperature is a maximum. No evidence of embrittlement was found in tension or room temperature fracture toughness tests. Embrittlement was noted, however, in fracture toughness tests carried out at -50 and -100 F, which indicates that low temperature testing will be necessary for proper materials evaluation. The plane strain fracture toughness (K_{Ic}) of various heats of 4340 steel has been correlated with the weight percent sulfur and phosphorus in the steel.

A mechanism for tempered martensite embrittlement is proposed. Certain impurity elements, such as phosphorus, which are more soluble in ferrite than in cementite, will segregate in the ferrite adjacent to the cementite shortly after the cementite precipitation. This transient enrichment of ferrite by impurity elements will be embrittling when the cementite is in a platelet or filmy form, and particularly so in the region of the prior austenite grain boundaries, where the impurity content may be higher than average.

CONTENTS

INTRODUCTION

Because of the occurrence of brittle fracture in steel, it has been recognized for a number of years that strength level alone is not a sufficient criterion for selecting materials for use in critical applications. In order to supplement strength properties, some measure of toughness is often employed, such as the energy absorption in the Charpy V-notch bend impact test. It has generally been found that the higher the strength level of a steel, the lower the toughness as measured by the Charpy impact energy. This generalization is occasionally violated and particularly low values of toughness may be obtained for a steel of a given strength level either because of poor heat treatment or composition; experience has shown that such steels are prone to brittle fracture in service. Numerous examples of such failures have been reported.[1]

Impact testing has been quite successful in indicating a possibility of brittle behavior, one example being steels quenched and tempered in the 500 to 700 F range, the range of so-called 500 F or tempered martensite embrittlement. While no indication of brittle behavior is obtained from a regular tension test, impact tests often reveal a pronounced minimum in the range of 500 to 700 F if room temperature impact energy is plotted against tempering temperature. Since greater toughness can be obtained by tempering at lower or higher temperatures, this tempering temperature range is generally avoided for many steels.

Recently, fracture toughness testing has come into favor at the expense of Charpy testing, especially in the range of high strength levels, where the low values of Charpy energy make this test insensitive, and for sheet materials where full-size Charpy specimens cannot be obtained. The application of fracture mechanics to crack propagation in metals is based on extensions of the original Griffith theory of brittle fracture of glass by Irwin[2] and Orowan.[3] The current status of fracture toughness testing and recommended testing procedures have been presented in a series of reports by ASTM Committee E 24 on Fracture Testing of Metals[4] and elsewhere.[5-7] Different specimens may be used: edge or center-notched sheet or circumferentially notched round bar, loaded in tension; or single edge-notched rectangular specimens loaded in tension or bending. No matter what the specimen type, current practice dictates that the machined notch be extended into a crack, generally by fatiguing. K_{Ic}, the critical value of the stress-intensity factor under plane strain conditions, is generally reported as a measure of fracture toughness.

The purpose of this report is to compare fracture toughness with impact properties in a case where brittleness has been well documented by Charpy impact testing, specifically 4340 steel quenched and tempered in the 500 F embrittlement range.

MATERIAL AND PROCEDURE

The 4340 steel used was taken from 1/8-inch-thick plate with the following chemical analysis: 0.41 C, 0.72 Mn, 0.33 Si, 1.83 Ni, 0.78 Cr, 0.26 Mo, 0.015 P, and 0.009 S. Tensile, impact, and fracture toughness properties were

measured for this steel tempered in 50-degree increments through the embrittlement range, generally 400 F to 700 F. Tension and fracture toughness tests were conducted over a range of temperatures from +200 F to -100 F. The annealed as-received plate was sheared oversized into longitudinal smooth and fracture toughness tension specimen blanks. These blanks were heat treated as follows: normalized for one hour at 1600 F; austenitized at 1550 F for one hour and oil quenched; and tempered for one hour. After heat treatment the blanks were then ground to an approximate thickness of 0.1 inch.

Smooth tensile properties were obtained using a pin-loaded specimen with a 0.5-inch width and a 2.0-inch gage length. The ASTM-recommended fracture toughness specimen measured 3 inches wide by 12 inches long. A 1.0-inch center notch was electrically machined into the specimen and extended to approximately 1.2 inches by tension-tension fatiguing at a maximum stress of 10 or 25 percent of the tensile yield strength. No appreciable differences in fracture toughness values were noted for duplicate specimens using either maximum fatiguing stress. However, the higher stress did result in some shear lip formation. The slow growth of this notch was monitored continuously during testing with an electric-potential technique.[8] Plane strain fracture toughness values K_{Ic} were calculated for the load corresponding to a deviation from linearity between the applied load and electric-potential curve. The deviations in linearity were either smooth or stepped.

Smoothly varying curves, indicating continuous crack growth to fracture, occurred at room and +200 F testing temperatures. Ideal plane strain K_{Ic} conditions did not exist because of the relatively large size of the plastic zone in comparison to the sheet thickness, which prevented a pop-in. It is recognized that the K_{Ic} values reported may be somewhat higher than would normally be expected from thicker sheet. The load at the point of nonlinearity can be readily determined within ± 5 percent which results in the same percentage change in K_{Ic}.

A stepped curve generally showed a pop-in followed by a period of crack arrest with increasing load for the -50 and -100 F test temperatures. At these temperatures, the specimen dimensions were suitable for plane strain conditions.[7] Several such pop-ins may occur before fracture. To insure that the first step was a pop-in valid for K_{Ic} calculations, a specimen tempered at 400 F was fatigued at room temperature and then pulled at -100 F until the first step occurred followed by a slight increase in load. The test was stopped and the specimen was again fatigued (room temperature) at the initial stress level and finally fractured at room temperature. The fracture surface is shown in Figure 1 where the pop-in extension can be easily seen.

The following equation for K_{Ic} was used:

$$K_{Ic} = \sigma_I \left[W \tan\left(\frac{\pi a_o}{W} + \frac{K_{Ic}^2}{2W\sigma_{ys}^2} \right) \right]^{1/2}$$

where σ_I = gross section stress at deviation

W = specimen width

a_o = 1/2 crack length at deviation

σ_{ys} = 0.2% tensile yield stress

The critical stress-intensity factor at instability, K_c, was also calculated from the same equation using one-half the crack length and the gross section stress at failure instead of at deviation.

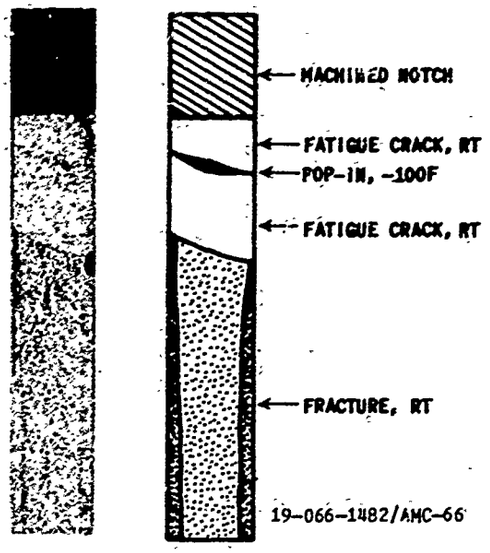

Figure 1. PLANE STRAIN CRACK EXTENSION AT -100 F. CENTER-NOTCHED SPECIMEN TEMPERED AT 400 F. 5X.

Subsize Charpy impact specimens, 0.097 inch wide by 0.394 inch deep, were machined from the fracture toughness specimens tested at room temperature. The transition temperatures, taken as the lowest temperature at which the fracture is 100 percent fibrous, will be somewhat lower than that obtained from a standard 0.394-inch-square Charpy impact specimen.[9] All mechanical testing procedures followed ASTM recommendations. Test temperatures were obtained by using radiant heating lamps or dry ice in alcohol. Companion tests conducted at room temperature in alcohol showed no effect of this environment upon crack growth.

PREVIOUS WORK

Embrittlement after tempering at 500 to 700 F is generally shown by a minimum in a plot of the room temperature Charpy impact energy versus tempering temperature, and has been reported by a number of investigators.[10-13] Other investigators have noted minima in room temperature notch tensile[14] and torsion impact tests.[15]

Ripling[16] showed the importance of test temperature as a criterion for evaluating tempered martensite embrittlement. In unnotched tensile tests on 1340 steel, he showed no discontinuity in room temperature tensile properties over a range of tempering temperatures up to 1200 F. Reducing the testing temperature to -196 C (-320 F) showed no evidence of embrittlement by yield or tensile strength. While no discontinuity in reduction of area and fracture stress had been noted at room temperature, a minimum in these properties at 500 F was noted at low temperatures. Apparently Rickett and Hodge[12] were the first to show by impact testing carried out over a range of temperatures that tempered martensite embrittlement is a manifestation of the change in transition temperature with tempering temperatures.

With the acceptance of fracture toughness testing, considerable data have been generated on the effect of tempering temperature (or strength level) on fracture toughness in 4340 and other high-strength steels. Hays and Wessel[17]

reported properties of 4340 over a range of test temperatures and tempering temperatures, although they intentionally avoided the 500 F embrittlement range. Backofen and Ebner[18] were concerned with the effect of processing history on fracture toughness of 4340 steel. No clear evidence of embrittlement was observed in their room temperature tests. Amateau, Hanna and Steigerwald[19] reviewed data on fracture toughness of 4340 steel. Data consolidated from several sources showed no evidence of 500 F embrittlement, either in room temperature or low temperature tests. In a later report, Amateau and Steigerwald[20] reported 500 F embrittlement in single edge-notched and notch bend specimens, but not with surface crack or center-notched tensile specimens. Lauta and Steigerwald[21] later studied the tensile and fracture toughness of 4340 steel as a function of tempering temperature and test temperature, and attempted to relate K_{Ic} to the strain hardening exponent. No simple relationship was evident.

Baker, Lauta, and Wei[22,23] reported fracture toughness of 4340 over a range of tempering temperatures. For both air-melted and consumable electrode vacuum-remelted steel they showed that K_{Ic} was relatively constant from 400 to 600 F, but increased sharply with further tempering. Banerjee[24,25] investigated air-melted and vacuum-induction-remelted 4340 steel. Fracture toughness was based on percentage shear in center-notched fatigue-cracked specimens and K_c (plane stress) values were reported. In the vacuum-induction-remelted steel, a minimum in toughness at 600 F was found. For the air-melted steel, a gradual increase in fracture toughness up to 800 F was found, although with considerable scatter in the 200 to 600 F range. The difference was attributed to the weakening effect of the inclusion-matrix interfaces in the air-melted steel.

These data on fracture toughness of 4340 steel from a number of sources show a somewhat contradictory pattern. It should be kept in mind, of course, that some of the data were generated using fracture toughness testing procedures which are not optimal by today's standards. Some investigators showed no evidence of 500 F embrittlement, with the fracture toughness increasing smoothly with increasing tempering temperatures. Other investigations showed some manifestation of embrittlement by a region of relatively constant toughness in the 500 to 700 F range but with the toughness increasing rapidly at higher temperatures, or in some cases, by an actual minimum in toughness. Composition (or melting practice) was a factor in one case, as was the type of specimen used to determine fracture toughness. Almost all the results are for room temperature tests. This is somewhat surprising, in view of the fact that tempered martensite embrittlement is generally recognized to be a manifestation of the change in transition temperature with tempering temperatures.

The mechanism of 500 F embrittlement has not yet been determined. Grossman[10] noted that the fracture surfaces of embrittled steels contained many bright, intercrystalline facets. From metallographic observations, he concluded that a ferrite grain boundary network was responsible for the embrittlement, and not retained austenite, which had been an earlier view. Klingler et al.[13] observed that embrittlement is a time-and-temperature-dependent phenomenon and is associated with the early stages of precipitation of cementite from martensite. They felt that localized precipitation of cementite at prior austenite grain boundaries and the ferrite network surrounding

this cementite was probably the cause of the embrittlement. It has also been suggested by Lement, Averbach, and Cohen[26] that a continuous carbide film at martensite plate boundaries forming in this temperature range could be the cause of embrittlement. Nakashima and Libsch[27] found that tempering by induction heating avoided tempered martensite embrittlement and also tended to form globular carbides at the start of the third stage of tempering. The association of embrittlement with the precipitation of cementite is also confirmed by the effect of silicon on tempering. Allten and Payson,[28] Shih, Averbach, and Cohen,[29] and Altstetter, Cohen, and Averbach[30] showed that an increase in silicon content raises the temperature at which cementite formation begins, and also raises the temperature for the minimum in impact energy.

Thermomechanical treatments, such as the formation of martensite in cold-worked austenite, have been found to alleviate the tendency toward embrittlement on tempering by shifting the impact transition curve to lower temperatures.[31]

Considerable evidence has been gathered, especially by Capus,[32-34] that impurity elements play an important role in controlling embrittlement. High purity steel shows no tempered martensite embrittlement, and the transition temperature decreases continuously with increasing tempering temperature. Additions of certain impurity elements, P, As, Sb, Sn, N, and Si, may lower the supertransition energy level and give rise to a maximum in the transition temperature at some intermediate tempering temperature.

Recently, transmission electron microscopy has been used to study the structure of steel tempered in this range. Baker et al.[22] noted that the improvement in toughness on tempering beyond the 500 F embrittlement range was associated with a spheroidization of carbide particles at martensite and twin boundaries, recovery in the high dislocation density array, and elimination of the twin boundaries. The actual embrittlement was aided by preferential paths for crack propagation provided by the carbide films.

Somewhat different conclusions were reached by Banerjee.[24,25] He concluded that tempered martensite embrittlement (as well as temper brittleness, which occurs in certain steels at about 1000 F) was associated with the simultaneous resolution of a metastable precipitate and reprecipitation of a more stable precipitate. He felt that a higher dislocation density, together with locking of the dislocation intersections and jogs by the precipitate, was the cause of the embrittlement.

Bucher et al.[35] have recently studied the structure of high-strength steels by electron fractography. They showed that the fracture surfaces of Charpy impact specimens tempered in the embrittlement range contained high proportions of grain boundary fracture (up to 40%) whereas the fracture surfaces of specimens tempered below and above this range were predominantly dimpled rupture or cleavage. These results strikingly confirmed the relationship between tempered martensite embrittlement and grain boundary fracture.

RESULTS

The subsize Charpy V-notch impact results are shown in Figure 2. The energy and the fibrosity in the fracture are plotted versus testing temperature for tempering temperatures of 400, 450, 500, 550, 600, 650, and 700 F. In Figure 3 the room temperature energy is plotted versus tempering temperature. Tempered martensite embrittlement is evident by the minimum extending from 500 to 650 F.

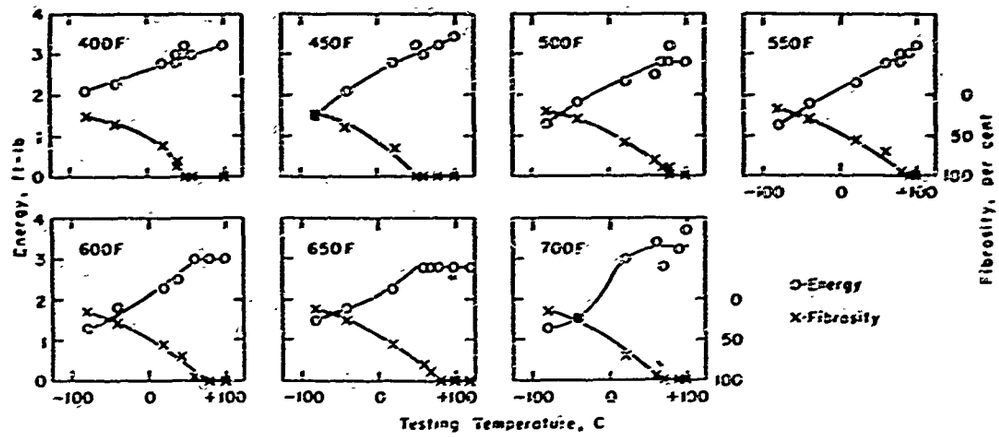

Figure 2. IMPACT ENERGY AND FRACTURE APPEARANCE AS A FUNCTION OF TESTING TEMPERATURE FOR VARIOUS TEMPERING TEMPERATURES.
19-066-855/AMC-66 ONE-QUARTER WIDTH. STANDARD DEPTH CHARPY SPECIMENS.

The transition temperature was determined for each tempering temperature, using as a criterion the lowest temperature at which the fracture appearance is 100 percent fibrous. This is plotted in Figure 4. It can be seen that the transition temperature is a maximum in the region of embrittlement. If some temperature above the transition temperature were used as a reference instead of room temperature, embrittlement would be much less evident. This is shown in Figure 5 where the energy at a test temperature of 100 C is plotted versus tempering temperature, and the curve is quite flat.

The energy values in Figures 2, 3, and 5 were determined on standard depth, quarter-width specimens. The energy for a full-size (0.394-inch square) Charpy bar at a given percent fibrosity can be approximated by multiplying the energy values by four.[9] However, the transition temperature and the whole transition region is shifted to lower temperatures with reduced width specimens. For the size of bar used and in this tempering temperature range for 4340 steel, the results of Fahey and Kula[9] show that the transition temperature is reduced about 30 to 60 C.

Standard smooth bar tensile properties determined over a range of tempering temperatures from 400 to 700 F are plotted in Figure 6. These show that the tensile strength decreased steadily over this temperature range, while the yield strength is almost constant between 400 and 600 F, and then decreases.

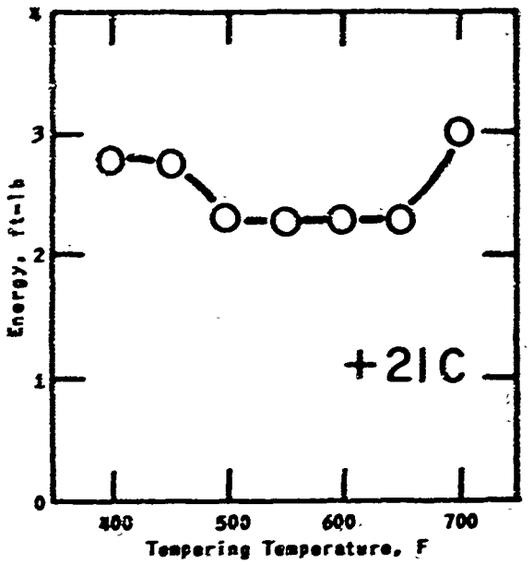

Figure 3. ROOM TEMPERATURE IMPACT ENERGY AS A FUNCTION OF TEMPERING TEMPERATURE. ONE-QUARTER WIDTH, STANDARD DEPTH CHARPY SPECIMENS.

19-066-856/AMC-66

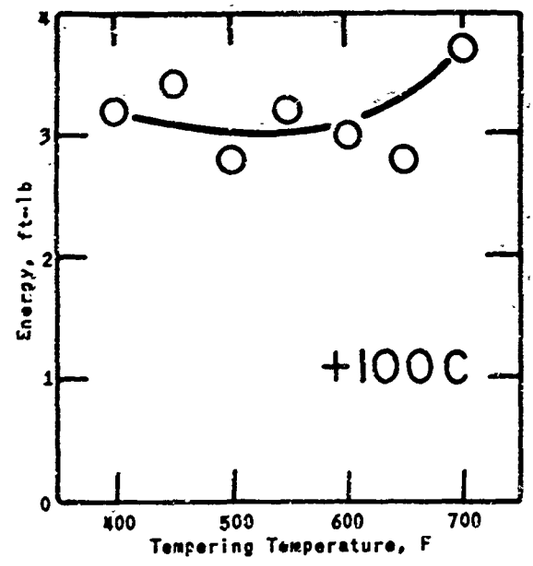

Figure 5. IMPACT ENERGY AS A FUNCTION OF TEMPERING TEMPERATURE FOR TESTS CONDUCTED AT +100 C. ONE-QUARTER WIDTH, STANDARD DEPTH CHARPY SPECIMENS.

19-066-858/AMC-66

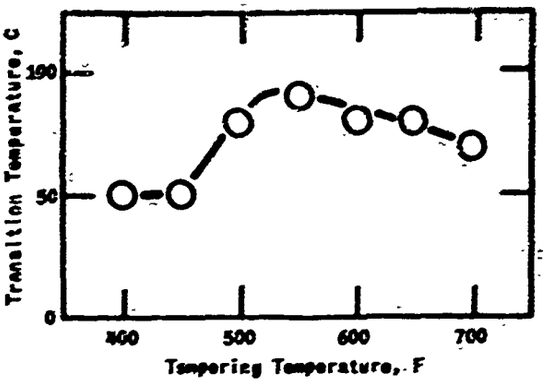

Figure 4. EFFECT OF TEMPERING TEMPERATURE ON (100 PERCENT FIBROSITY) CHARPY TRANSITION TEMPERATURE. ONE-QUARTER WIDTH, STANDARD DEPTH CHARPY SPECIMENS.

19-066-857/AMC-66

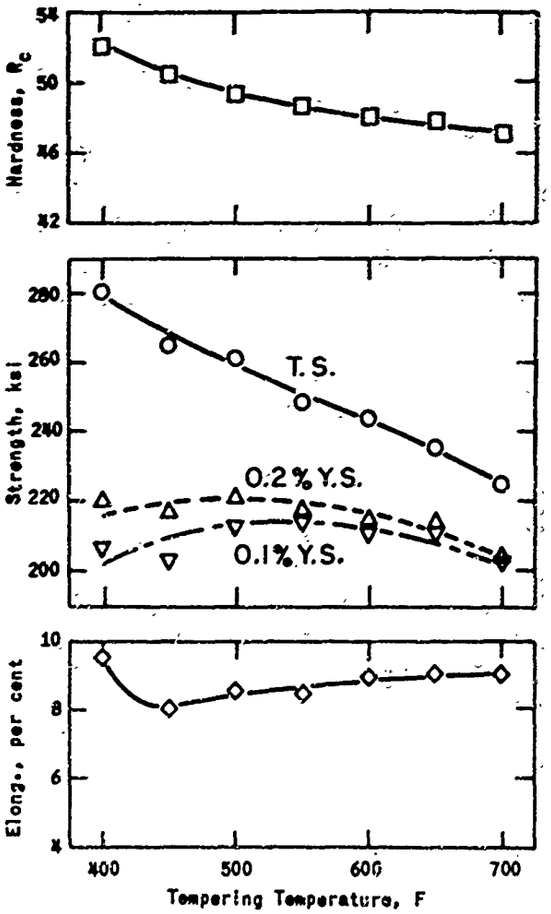

Figure 6. EFFECT OF TEMPERING TEMPERATURE ON ROOM TEMPERATURE HARDNESS AND TENSILE PROPERTIES.

19-066-859/AMC-66

The elongation shows little change. The Rockwell C hardness, also plotted in Figure 6, shows a decrease over this range.

The yield and tensile strengths were determined over a range of test temperatures for several tempering temperatures in order to subsequently determine the fracture toughness. These results are plotted in Figure 7, and show that the strength increases as the test temperature decreases.

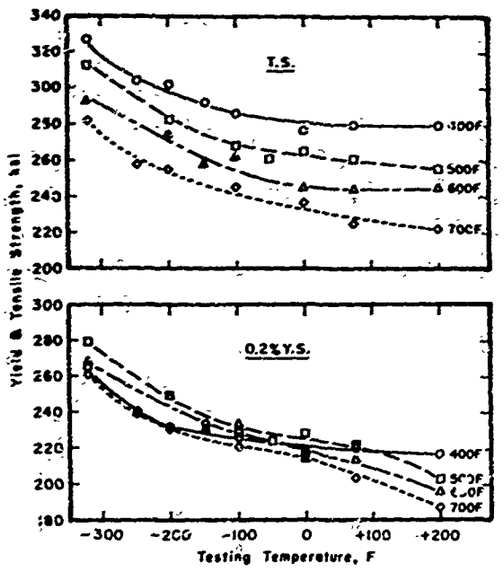

Figure 7. EFFECT OF TEMPERING AND TESTING TEMPERATURE ON THE YIELD AND TENSILE STRENGTH

19-066-860/AMC-66

Fracture toughness values, both plane strain K_{Ic} as well as plane stress K_c, were determined over a range of test temperatures between -190 and +200 F for tempering temperatures between 400 and 700 F. The results in Figure 8 show that the K_c values drop sharply with decreasing test temperature, especially for the higher tempering temperatures. The plane strain fracture toughness shows much less of a change with temperature, and for the lower tempering temperatures is almost independent of test temperature.

The percent shear in the fracture has sometimes been used as a measure of fracture toughness. The results in Figure 9 for shear measurements at a distance two times the specimen thickness from the edge of the specimen show that the percent shear decreases rapidly below room temperature for most tempering temperatures. The K_c values qualitatively follow the change in percent shear.

The values of K_{Ic} and K_c from Figure 8 are plotted versus tempering temperature in Figure 10. The results for +200 and +80 show no evidence of embrittlement with the toughness increasing steadily throughout the embrittlement range. The trends at -50 and -100 F are quite different, however. To supplement the original data, some additional samples were tempered over the range 400 to 700 F and at 800 and 900 F. At these test temperatures, the fracture toughness decreases slightly as the tempering temperature is increased beyond 400 F, goes through a minimum in the embrittlement range, and then rises at 800 and 900 F.

These trends are shown again in Figure 11, where the fracture toughness is plotted versus the yield strength. While the results for +200 F and +80 F temperature show the usual trend of decreasing toughness with increasing strength, the results for -50 and -100 F show an evidence of embrittlement in that the toughness is a minimum at 215 to 225 ksi yield strength.

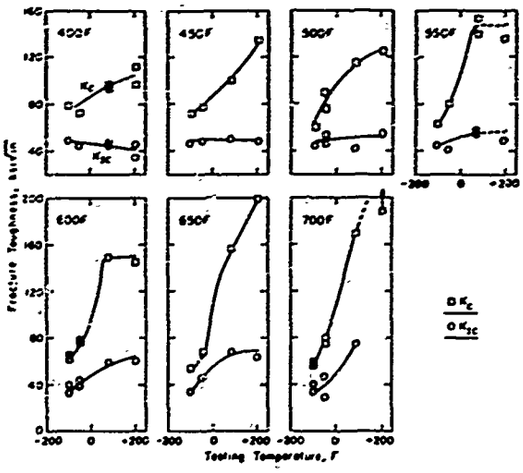

Figure 8. PLANE STRESS AND PLANE STRAIN FRACTURE TOUGHNESS AS A FUNCTION OF TESTING TEMPERATURE FOR VARIOUS TEMPERING TEMPERATURES

19-066-1487/AMC-66

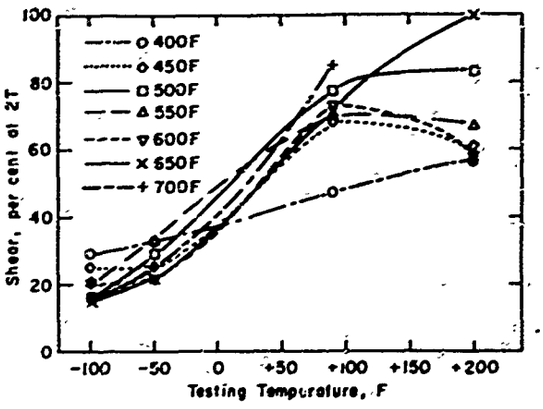

Figure 9. EFFECT OF TEST TEMPERATURE ON PERCENT SHEAR FRACTURE FOR VARIOUS TEMPERING TEMPERATURES. MEASUREMENT AT 2T FROM EDGE.

19-066-1488/AMC-66

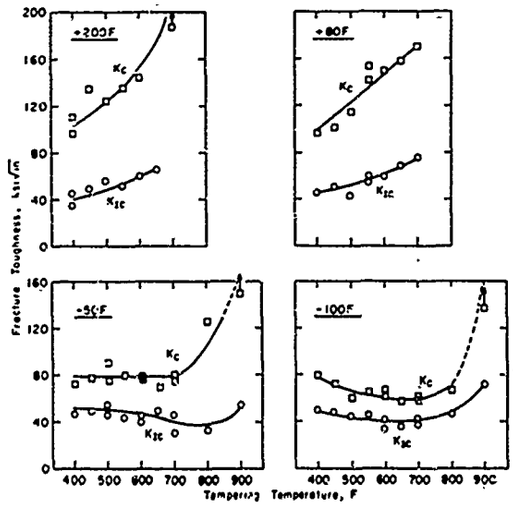

Figure 10. PLANE STRESS AND PLANE STRAIN FRACTURE TOUGHNESS AS A FUNCTION OF TEMPERING TEMPERATURE FOR SEVERAL TEST TEMPERATURES

19-066-1484/AMC-66

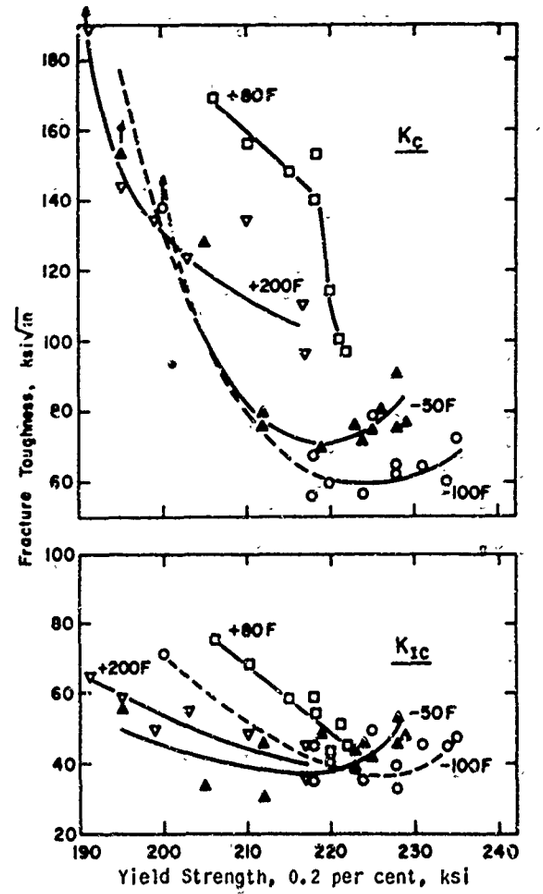

Figure 11. EFFECT OF YIELD STRENGTH ON PLANE STRESS AND PLANE STRAIN FRACTURE TOUGHNESS FOR SEVERAL TESTING TEMPERATURES

19-066-1483/AMC-66

DISCUSSION

Fracture Toughness

The major question to be answered is whether fracture toughness testing can show the presence of tempered martensite embrittlement. The room temperature results plotted in Figure 10 show no embrittlement; these results and those of several other investigations are summarized in Figure 12. The chemical compositions of the 4340 steels used in these investigations are given in Table I. While the values of K_{Ic} vary over quite a range, no marked minimum in toughness is evident. On the other hand, results for test temperatures below room temperature shown in Figure 10 do show unmistakable evidence of embrittlement by a minimum in toughness in the range 600 to 700 F. The answer is clear that tempered martensite embrittlement can be demonstrated by fracture toughness testing, although a testing temperature below room temperature may be necessary.

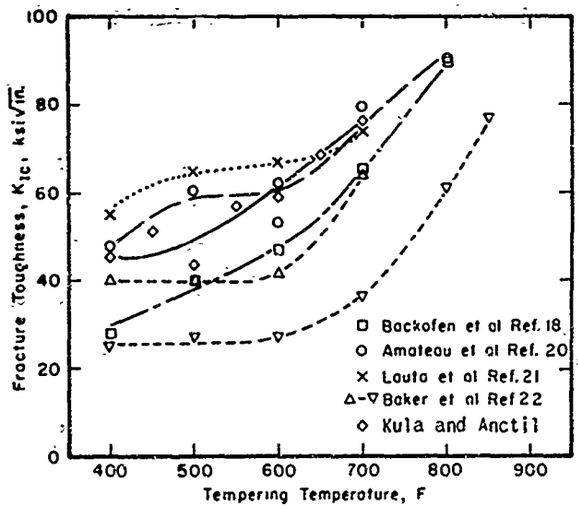

Figure 12. FRACTURE TOUGHNESS AS A FUNCTION OF TEMPERING TEMPERATURE FOR 4340 STEEL FROM SEVERAL DIFFERENT INVESTIGATIONS.

19-066-1486/AMC-66

Table I. CHEMICAL COMPOSITIONS OF THE 4340 STEEL SHOWN IN FIGURES 12 AND 13

	Composition, weight percent							
	C	Mn	Ni	Cr	Mo	Si	P	S
Lauta, et al Ref. 21	.43	.84	1.78	.78	.26	.27	0.006	.005
Amateau, et al " 20	.43	.65	1.85	.82	.26	.30	.010	.005
Baker, et al " 22	.43	.77	1.16	.73	.26	.27	.009	.008
Kula and Anctil	.41	.72	1.83	.78	.26	.33	.015	.009
Backofen, et al Ref. 18	.39	.77	1.75	.81	.22	.30	.012	.015
Baker, et al " 22	.39	.74	1.79	.89	.26	.27	.019	.026

This should not be too surprising since it is well known from Charpy impact test results that this embrittlement is primarily a result of the high transition temperatures in the embrittlement region. The observed severity of embrittlement (i.e., the magnitude of the energy drop on an energy-tempering temperature plot) depends on several factors relating to the surface resulting from the three-dimensional plot of energy (or toughness value), test temperature, and tempering temperature. These are: the reference or test temperature and its relation to the transition temperature; the rate of change of transition temperature with tempering temperature; the rate of change of energy value with tempering temperature, both above and below the transition; and the sharpness of the transition temperature region. A narrow transition region, a large change of transition temperature with tempering temperature, and a test temperature lying within the range of transition temperatures will all tend to give a greater manifestation of embrittlement.

While the transition region in the Charpy test may not be particularly sharp for high strength steels, it does vary with tempering temperature (Figure 4) and lies above room temperature for certain tempering treatments. Unfortunately, there is little information on transition temperatures for fracture toughness values. A transition region does exist for plane stress fracture toughness K_c (Figure 8). Presumably this can be accounted for by the variation in the percent shear in the fracture over this same temperature range (Figure 9), just as the Charpy impact energy values in the transition region are related to the volume of plastically deformed material. But although the plane strain fracture toughness K_{Ic} does vary with test temperature (Figure 8), the transition is much less sharp, if a transition in its true meaning does exist at all. Bucher et al.[35] did report changes in the relative amounts of cleavage, dimpled rupture, and grain boundary fracture in Charpy impact specimens tested over a range of tempering and test temperatures, and in slow bend specimens at several tempering temperatures. Preliminary results on electron fractography of the fracture toughness specimens used in this investigation confirmed the results of Bucher. Thus it may ultimately be possible to relate a transition in fracture toughness to changes in the micromechanics of fracture.

The deleterious effects of certain impurity elements which are associated with tempered martensite embrittlement were mentioned earlier. These elements, such as phosphorus, are present in solid solution, and influence both the toughness level and the transition temperature. Sulfur, on the other hand, which does not cause tempered martensite embrittlement, is present in the form of second-phase sulfide particles. These sulfide particles reduce the impact energy level, but have only a small effect on transition temperature, as the results of Hodge, Frazier, and Boulger have shown.[36] Wei[23] has demonstrated the deleterious effect of sulfur on fracture toughness in high purity 4335 steel.

Both sulfur and the other impurity elements are present in commercial steels. Recently, Gazza and Larson[37] related the supertransition impact energy level of 4340 steel, quenched and tempered at 950 F, to the sum of the weight percent of phosphorus and sulfur, and showed that the energy decreased as the impurity content increased. The room-temperature K_{Ic} plane

strain fracture toughness values summarized in Figure 12 are replotted in Figure 13 versus the sum of the weight percent sulfur and phosphorus (from Table I) for 400 and 700 F tempering temperatures. The fracture toughness determinations were made by different investigators on different type specimens, and the effect of other elements such as carbon, oxygen, and the trace impurities are not considered so that there is considerable scatter in data. However, it is clear that the results of these various investigations are consistent and that both sulfur and phosphorus have a strong effect on reducing fracture toughness.

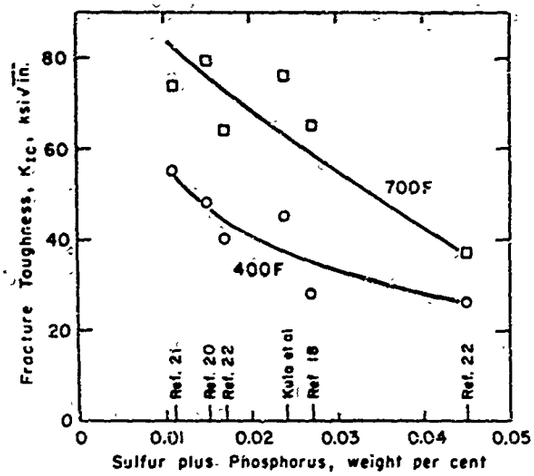

Figure 13. VARIATION OF FRACTURE TOUGHNESS WITH SULFUR PLUS PHOSPHORUS CONTENT FOR 400 AND 700 F TEMPERS.

19-066-1485/AMC-66

Mechanism of Embrittlement

Although it was not the purpose of this study to try to determine the mechanism of tempered martensite embrittlement, some general comments can be made. The early results of Ripling[16] demonstrated quite clearly that this embrittlement is associated with a discontinuity in ductility, but not in tensile flow properties. Under appropriate conditions of temperature, stress state, and strain rate, this reduced ductility can manifest itself in reduced toughness. Accordingly, the cause of tempered martensite embrittlement should be sought in some factors which reduce ductility rather than influence strength.

From the many observations that have been made on embrittled steels, several appear to be significant:

1. When embrittled, the fracture surface shows a large amount of failure along prior austenite grain boundaries. This was recognized by Grossman[10] and Capus,[32] and has recently been confirmed by Bucher et al.[35] who made quantitative measurements of fracture surfaces by electron fractography.

2. Embrittlement does not occur in high purity steels. It is promoted by certain impurity elements--phosphorus, arsenic, antimony, tin, nitrogen, and silicon, as has been shown by Capus.[32-34]

3. Embrittlement is associated with the start of the third stage of tempering, where cementite starts to form at the expense of epsilon carbide, and it appears to follow the same time-temperature relations as the tempering.[13] When silicon is added to steel, the start of the third stage of tempering is retarded and the embrittlement range is shifted to higher temperatures.[28-30] At this stage of tempering, the cementite is filmy or platelet in appearance and tends to form preferentially at martensite platelet boundaries or at prior austenite grain boundaries.[13,26] If the initial precipitation of the cementite in a platelet or filmy form can be avoided, as

with tempering by induction heating where the cementite is globular, tempered martensite embrittlement can be avoided.[27] During this same stage of tempering, the martensite matrix contains a high dislocation density, while at higher temperatures, there is some recovery and elimination of twin boundaries in the martensite.[22,24,25] This observation on the structure in the martensite may or may not be pertinent to the problem of embrittlement.

Most of the explanations for tempered martensite embrittlement have embodied some but not all of the above features. Generally, the importance of the impurity elements has been overlooked. Capus[34] did recognize the necessity of all three of these observations, and suggested that perhaps the structures produced in this embrittling range are particularly sensitive to the presence of impurity elements. An interaction between segregated impurity elements and cementite films or perhaps with the defect structure of the martensite was postulated. Bucher et al. also suggested that the impurities might segregate in the ferrite in the vicinity of the cementite plates.[35] What is suggested in the following is a mechanism whereby certain impurity elements can segregate in the vicinity of cementite and, thereby, cause embrittlement.

When a quenched steel is tempered, the cementite that forms initially inherits the alloy content of the martensite, which in turn is inherited from the austenite. At the low temperatures at which epsilon carbide and the first cementite form, it is primarily the interstitial carbon which can diffuse while the larger substitutional elements remain in place. As tempering proceeds for longer times and to higher temperatures, the alloying elements can diffuse and redistribute themselves according to an equilibrium distribution ratio, given by the phase diagram, between the ferrite matrix and the cementite or between the ferrite and an alloy carbide which may subsequently form. This has been shown by Kuo,[38] who determined the chemical composition of electrolytically extracted carbides after various tempering times. For example, in a 0.51% C-3.13% Cr steel, tempered at 560 C, the chromium content of the carbide phase had risen to about 7 percent after one hour tempering and approached 18 percent, the saturation value in cementite, in about 10 hours. The cementite was replaced by Cr_7C_3 on further tempering, and the chromium content of the carbide phase continued to increase to almost 40 percent in about 50 to 100 hours. This redistribution will take place with any alloying element at a sufficiently high temperature, with those elements that prefer the carbide phase diffusing to the carbide and other elements diffusing into the ferrite away from the carbide. There is a scarcity of information on distribution ratios between ferrite and carbides, but it is known from the work of Kuo[38] and others[39] that strong carbide formers such as chromium, molybdenum, and tungsten segregate in the cementite by replacing iron atoms, while other elements such as silicon and phosphorus probably tend to dissolve more in the ferrite.[40] No information exists for tin, arsenic, and antimony, the other elements which reportedly cause tempered martensite embrittlement, but they probably prefer the ferrite since the elements replacing iron in cementite seem to be the transition elements. Nitrogen, which can replace carbon in cementite, may be an exception.

When cementite has formed and tempering is continued for longer times or at higher temperatures, these embrittling elements will start to diffuse out of the cementite into the surrounding ferrite. This process can be visualized more clearly by referring to Figure 14, which is a schematic drawing of the ferrite plus cementite phase field of an Fe-M-C alloy, where M is an element which dissolves more readily in ferrite than cementite.

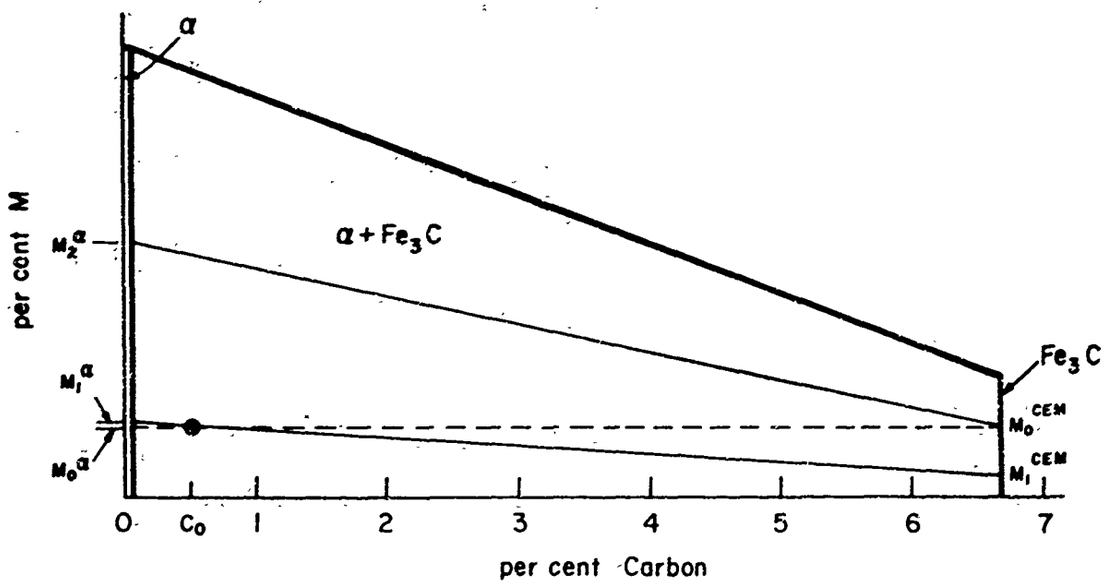

19-066-1489/AMC-66 Figure 14. IRON CORNER OF SCHEMATIC Fe-M-C PHASE DIAGRAM

The composition of the steel is shown by the solid circle, with an M content of M_0 and C content of C_0. Tie lines, or iso-activity lines, in this two-phase field are M^{α}_1-M_1^{cem} and M^{α}_2-M_0^{cem}. On initial formation of the cementite, at temperatures too low for the diffusion of M, the M content of the ferrite and cementite will be the same, M^{α}_0, and M_0^{cem}, and equal to M_0. The activity of M in the cementite will be much higher than in the ferrite, however.

The equilibrium M contents for this composition are given by the ends of the tie line through M_0C_0, namely M^{α}_1 and M_1^{cem}. When the cementite precipitation is completed and tempering proceeds, M will diffuse into the ferrite because of the higher M activity in cementite. Cementite of a composition M_0^{cem} is in equilibrium with ferrite of a composition M^{α}_2, so the M content at the interface will quickly rise to a value about midway between M^{α}_0 and M^{α}_2. This transient enrichment of ferrite by M near the interface would persist, with the enriched zone gradually widening and the interface composition gradually decreasing until, at higher temperatures, the cementite becomes impoverished in M and the concentration gradient in the ferrite is evened out, at which time equilibrium compositions will be attained.

The question arises as to whether there will be sufficient diffusion of alloying elements at the low temperatures at which embrittlement occurs.

A measure of the distance an element can diffuse into the ferrite, X, can be approximated by $X = \sqrt{Dt}$, where D is the diffusion coefficient and t the time. Using a diffusion coefficient of 7.1×10^{-3} exp-(40,000/RT) for phosphorus in ferrite, which was determined at higher temperatures,[41] one can calculate that a phosphorus atom could diffuse a distance of 18 A in one hour at an embrittling temperature of 600 F. Whether or not this is a reasonable amount of diffusion can be judged by comparing with data for tempering of chromium steels. The results of Kuo[38] show that there was sufficient diffusion of chromium in one hour at 560 C to raise the chromium content of cementite from 3.13 to about 7 percent. Under these conditions, and with $D = 3 \times 10^{4}$ exp-(82,000/RT),[42] one can calculate a distance of 16 Å, about the same as for phosphorus at 600 F. Even though these values of the diffusion coefficients are not strictly valid for an alloyed steel with a high dislocation density, they do show that considerable enrichment of the ferrite adjacent to cementite is possible. On prolonged tempering these transient segregations would disappear because of impoverishment of the cementite and the evening out of the concentration gradient in the ferrite, as mentioned earlier, and spheroidization of the cementite would occur as well.

The next question to be answered is why such a segregated region would be embrittling. It is possible that these elements lower the interfacial energy between ferrite and cementite, thus providing a weak interface. Also, phosphorus and silicon are two of the most potent substitutional solid solution strengthening elements in ferrite, far more potent than the transition elements.[43] Thus a small amount could have a strong effect on inhibiting dislocation motion in the immediate vicinity of the interface. It is also well known that phosphorus contents of the order of 0.1% in high purity iron alloys can have an embrittling effect.[44] If the carbide particles were spheroidal, the effect of the surrounding segregated regions might be to increase the effective size of the carbide, which would not be particularly embrittling. Also separation at the interfaces would not provide a continuous path for a crack. If the cementite is filmy or platelet in form, the adjoining segregated region would have the same shape. Under appropriate stress conditions, a crack that would initiate in the cementite could propagate easily over rather large distances in this region parallel to the interface and hence reach a critical size for unstable growth. It should be noted that in the model that is suggested here, the ferrite surrounding this cementite is stronger and less ductile than the matrix ferrite, in contrast to earlier models which believed that this ferrite region was softer than the rest of the ferrite.

The final question is why intergranular failure along prior austenite grain boundaries is prevalent in embrittled steels. Earlier writers have suggested that the prior austenite grain boundaries are preferential sites for cementite precipitation. Precipitation occurs earlier here, and the cementite particles are larger than inside the prior austenite grains, and are probably continuous. Thus any cracks would be longer at these locations.

It is also possible that the average impurity content of the austenite grain boundaries is high because of grain boundary segregation. Grain boundary segregation of phosphorus in ferrite has been demonstrated by Inman and Tipler.[45]

An increased phosphorus content at austenite grain boundaries would lead to a higher initial phosphorus content in the grain boundary cementite, and in turn to a still higher content in the ferrite at the interface.

In summary, the proposed mechanism is as follows: cementite inherits the impurity content of the martensite. At a sufficiently high temperature, after completion of the cementite precipitation in a platelet or filmy form, alloying elements in the ferrite and cementite will tend to diffuse and redistribute themselves according to an equilibrium distribution ratio. For those elements which have a higher solubility in ferrite than in cementite, this will lead to a transient enrichment of these elements in the ferrite near the cementite interface. When the cementite is in a platelet or filmy form, this region will allow an easy path for crack propagation. This process will be intensified at the prior austenite grain boundaries, where the cementite may be continuous or the platelets larger, and where the impurity content may be highest as a result of grain boundary segregation during austenitizing.

From the limited data that exist, this process seems feasible at least for phosphorus. Unfortunately, there appears to be no quantitative data on distribution coefficients between ferrite and cementite for phosphorus or any of the other elements that are known to cause tempered martensite embrittlement.

SUMMARY

Mechanical properties were determined for 4340 steel quenched and tempered through the range of tempered martensite or 500 F embrittlement and for a range of test temperatures.

Unnotched tensile properties showed a smooth variation of yield and tensile strengths and ductility over testing temperatures ranging from -320 to +200 F.

One-quarter width, standard depth Charpy V-notch impact specimens were tested from -80 to +100 C. Room temperature tests showed embrittlement in the tempering temperature range of 500 to 650 F. Transition temperatures were determined (that is, the minimum temperature at which the fracture was completely fibrous) and were found to be a maximum over this same range of tempering temperatures.

Plane strain, K_{Ic}, and plane stress, K_c, fracture toughness were determined on 3-inch-wide center-notched fatigue-cracked specimens. At room temperature and +200 F, the fracture toughness increased smoothly with increasing temperature or decreasing yield strength, and no evidence of tempered martensite embrittlement was evident. At test temperatures of -50 and -100 F, however, the fracture toughness shows a minimum in the embrittlement range. These results demonstrate that room temperature tests may not be sufficient to determine whether a steel is embrittled, and low temperature tests will be necessary. Plane strain fracture toughness, K_{Ic}, values for 4340 steels from

several different investigations were compared. It was found that the fracture toughness decreased as the sum of the weight percent sulfur plus phosphorus increased. Low impurity levels are necessary for the best toughness values.

A proposed mechanism for tempered martensite embrittlement is offered. Cementite when first formed inherits the alloy content of the martensite. As tempering proceeds, redistribution of the alloying elements will occur, and certain elements more soluble in ferrite will enrich the ferrite adjacent to the cementite. If the cementite is in a platelet or filmy form, this will provide a path for easy crack propagation, especially if these elements have a large strengthening effect on the ferrite or reduce the interfacial energy between ferrite and cementite. This process will occur preferentially at prior austenite grain boundaries, where the impurity content is highest and the cementite particles are largest or continuous.

ACKNOWLEDGMENT

The authors would like to express their appreciation for the helpful discussions with their colleagues at the U. S. Army Materials Research Agency, Frank Larson and Joseph Bluhm on fracture toughness testing, and Dr. Gordon Bruggeman on diffusion.

LITERATURE CITED

1. PARKER, E. R. *Brittle Behavior of Engineering Structures.* J. Wiley and Sons, Inc., New York, N. Y., 1957.

2. IRWIN, G. R. *Fracture.* Encyclopedia of Physics, Springer, Berlin, 6, 1958, p. 551.

3. GROWAN, E. *Fracture and Strength of Solids.* Report on Progress in Physics, Physical Soc., London, 12, 1949, p. 185.

4. AMERICAN SOCIETY for TESTING and MATERIALS, Special ASTM Committee on Fracture Testing of High-Strength Metallic Materials.

   First Report. *Fracture Testing of High-Strength Materials:* A Report of a Special ASTM Committee, ASTM Bulletin, 243, Jan. 1960, p. 29; 244, Feb. 1960, p. 18.

   Second Report. *The Slow Growth and Rapid Propagation of Cracks.* Materials Research and Standards, 1, May 1961, p. 389.

   Third Report. *Fracture Testing of High-Strength Sheet Materials.* Materials Research and Standards, 1, Nov. 1961, p. 877.

   Fourth Report. *Screening Tests for High-Strength Alloys Using Sharply Notched Cylindrical Specimens.* Materials Research and Standards, 2, March 1962, p. 196.

   Fifth Report. *Progress in Measuring Fracture Toughness and Using Fracture Mechanics.* Materials Research and Standards, 4, March 1964, p. 107.

5. CAMPBELL, J. E. *Current Methods of Fracture-Toughness Testing of High-Strength Alloys With Emphasis on Plane Strain.* DMIC Report 207, 1964.

6. SRAWLEY, J. E., and BROWN, W. F., Jr. *Fracture Toughness Testing Method.* Fracture Toughness Testing and Its Applications, ASTM STP No. 381, ASTM, Philadelphia, Pa., 1964, p. 133.

7. BROWN, W. F., Jr., and SRAWLEY, J. E. *Current Status of Plane Strain Crack Toughness Testing.* ASTM STP No. 410, ASTM, Philadelphia, Pa., 1967.

8. ANCTIL, A. A., KULA, E. B., and DiCESARE, E. *Electric Potential Technique for Determining Slow Crack Growth.* U. S. Army Materials Research Agency, AMRA TR 63-27, December 1963; also Proc. ASTM, 63, 1963, p. 799.

9. FAHEY, N. H., and KULA, E. B. *An Investigation of Subsize Charpy Impact Specimens.* Proc. ASTM, 63, 1963, p. 1147.

10. GROSSMANN, M. A. *Toughness and Fracture of Hardened Steels.* Trans. AIME, 167, 1946, p. 39.

11. SCHRADER, H., WIESTER, H. J., and SIEPMANN, H. *Embrittlement of Hardened Steels on Tempering at 250 to 400 C.* Archiv für das Eisenhuttenwesen, 21, 1950, p. 21.

12. RICKETT, R. L., and HODGE, J. M. *Notch-Toughness of Fully Hardened and Tempered Low-Alloy Steels.* Proc. ASTM, 51, 1951, p. 931.

13. KLINGLER, L. J., BARNETT, W. J., FROHMBERG, R. P., and TROIANO, A. R. *The Embrittlement of Alloy Steel at High-Strength Levels.* Trans. ASM, 46, 1954, p. 1557.

14. SACHS, G., LUBAHN, J. D., and EBERT, L. J. *Notched Bar Tensile Test Characteristics of Heat-Treated Low Alloy Steels.* Trans. ASM, 33, 1944, p. 340.

15. LUERSSEN, G. V., and GREENE, O. V. *Interpretation of Torsion Impact Properties of Carbon Tool Steel.* Trans. ASM, 23, 1935, p. 861.

16. RIPLING, E. J. *Tensile Properties of a Heat-Treated Low Alloy Steel at Subzero Temperatures.* Trans. ASM, 42, 1950, p. 439.

17. HAYS, L. E., and WESSEL, E. T. *The Fracture Toughness of 4340 Steel at Various Yield Strength Levels.* Applied Mater. Res., 2, 1963, p. 99.

18. BACKOFEN, W. A., and EBNER, M. L. *Metallurgical Aspects of Fracture at High Strength Levels.* Massachusetts Institute of Technology, Contract DA-19-020-ORD-5235, Final Report, WAL TR 310.24/5-4, 1963.

19. AMATEAU, M. F., HANNA, G. L., and STEIGERWALD, E. A. *Fracture Characteristics of Structural Metals.* U. S. Bureau of Naval Weapons, Contract Now-64-0186C, First Quart. Rpt., 1964.

20. AMATEAU, M. F., and STEIGERWALD, E. A. *Fracture Characteristics of Structural Metals.* U. S. Bureau of Naval Weapons, Contract Now-64-0186C, 1965.

21. LAUTA, F. J., and STEIGERWALD, E. A. *Influence of Work Hardening Coefficient on Crack Propagation in High-Strength Steels.* AFML-TR-65-31, 1965.

22. BAKER, A. J., LAUTA, F. J., and WEI, R. P. *Relationships Between Microstructure and Toughness in Quenched and Tempered Ultrahigh-Strength Steels.* Structure and Properties of Ultrahigh-Strength Steels, ASTM STP No. 370, ASTM, Philadelphia, Pa., 1963, p. 3.

23. WEI, R. P. *Fracture Toughness Testing in Alloy Development.* Fracture Toughness Testing and Its Applications, ASTM STP No. 381, ASTM, Philadelphia, Pa., 1964, p. 279.

24. BANERJEE, B. R. *Fracture Micromechanics in High-Strength Steels.* Structure and Properties of Ultrahigh-Strength Steels, ASTM STP No. 370, ASTM, Philadelphia, Pa., 1963, p. 94.

25. BANERJEE, B. R. *Embrittlement of High-Strength Tempered Alloy Martensites.* J. Iron Steel Inst., 203, 1965, p. 166.

26. LEMENT, B. S., AVERBACH, B. L., and COHEN, M. *Microstructural Changes on Tempering Iron-Carbon Alloys.* Trans. ASM, 46, 1954, p. 851.

27. NAKASHIMA, A., and LIBSCH, J. F. *Effect of Induction on 500 C Embrittlement.* Trans. ASM, 53, 1961, p. 753.

28. ALLTEN, A. A., and PAYSON, P. *The Effect of Silicon on the Tempering of Martensite.* Trans. ASM, 45, 1953, p. 498.

29. SHIH, C. H., AVERBACH, B. L., and COHEN, M. *Some Effects of Silicon on the Mechanical Properties of High-Strength Steels.* Trans. ASM, 48, 1956, p. 86.

30. ALTSTETTER, C. J., COHEN, M., and AVERBACH, B. L. *Effect of Silicon on the Tempering of AISI 43XX Steels.* Trans. ASM, 55, 1962, p. 287.

31. KULA, E. B., and DHOSI, J. M. *Effect of Deformation Prior to Transformation on the Mechanical Properties of 4340 Steel.* U. S. Army Materials Research Agency, WAL TR 630/22, June 1958; also Trans. ASM, 52, 1960, p. 321.

32. CAPUS, J. M. *L'Influence D'Oligo-Éléments Sur La Résilience Des Aciers Faiblement Alliés.* Trempés Et Revenus, Rev. de Métallurgie, 56, 1959, p. 181.

33. CAPUS, J. M., and MAYER, G. *The Influence of Trace Elements on Embrittlement Phenomena in Low-Alloy Steels.* Metallurgia, 62, 1960, p. 133.

34. CAPUS, J. M. *Carbide Precipitation, Impurity Elements, and The Embrittlement of High-Strength Martensitic Alloy Steels.* J. Iron Steel Inst., 201, 1963, p. 53.

35. BUCHER, J. H., POWELL, G. W., and SPRETNAK, J. W. *A Micro-Fractographic Analysis of Fracture Surfaces in Some Ultrahigh-Strength Steels.* Application of Fracture Toughness Parameters to Structural Materials, H. D. Greenberg, ed., Gordon and Breach Science Publishers, New York, N. Y., 1966, p. 323.

36. HODGE, J. M., FRAZIER, R. H., and BOULGER, F. W. *The Effects of Sulfur on the Notch Toughness of Heat-Treated Steels.* Trans. AIME, 215, 1959, p. 745.

37. GAZZA, G. E., and LARSON, F. R. *Impact Properties of Air- and Vacuum-Melted AISI 4340 Steel.* U. S. Army Materials Research Agency, AMRA TR 65-22, September 1965; also Trans. Quart., ASM, 58, 1965, p. 183.

38. KUO, K. *Carbides in Chromium, Molybdenum, and Tungsten Steels.* J. Iron Steel Inst., 173, 1953, p. 363.

39. BARRETT, C. S. *Structure of Metals.* 2nd Ed., McGraw-Hill Co. Inc., New York, N. Y., 1952, p. 246.

40. BAIN, E. C., and PAXTON, H. W. *Alloying Elements in Steel.* ASM, Metals Park, Ohio, 1961, p. 59.

41. GRUZIN, P. L., and MINAL, V. V. *Radiometric Study of Phosphorus Diffusion in Iron.* Phys. of Met. and Metallography, 16, 1963, p. 50.

42. GRUZIN, P. L. *Diffusion of Cobalt, Chromium, and Tungsten in Iron and Steel.* Doklady Akademii Nauk SSSR, 94, 1954, p. 681.

43. LACY, C. E., and GENSAMER, M. *The Tensile Properties of Alloyed Ferrites.* Trans. ASM, 32, 1944, p. 88.

44. HOPKINS, B. E., and TIPLER, H. R. *The Effect of Phosphorus on the Tensile and Notch-Impact Properties of High-Purity Iron and Iron-Carbon Alloys.* J. Iron Steel Inst., 188, 1958, p. 218.

45. INMAN, M. C., and TIPLER, H. R. *Grain-Boundary Segregation of Phosphorus in an Iron-Phosphorus Alloy and the Effect Upon Mechanical Properties.* Acta Met., 6, 1958, p. 73.

U. S. ARMY MATERIALS RESEARCH AGENCY
WATERTOWN, MASSACHUSETTS 02172

TECHNICAL REPORT DISTRIBUTION

Report No.: AMRA TR 67-03 January 1967 Title: Tempered Martensite Embrittlement and Fracture Toughness in 4340 Steel

No. of Copies	To
1	Office of the Director, Defense Research and Engineering, The Pentagon, Washington, D. C. 20301
20	Commander, Defense Documentation Center, Cameron Station, Building 5, 5010 Duke Street, Alexandria, Virginia 22314
1	Defense Metals Information Center, Battelle Memorial Institute, Columbus, Ohio 43201
1	Chemical Propulsion Information Agency, Applied Physics Laboratory, The Johns Hopkins University, 8621 Georgia Avenue, Silver Spring, Maryland 20910
	Chief of Research and Development, Department of the Army, Washington, D. C. 20310
2	ATTN: Physical and Engineering Sciences Division
	Commanding Officer, Army Research Office (Durham), Box CM, Duke Station, Durham, North Carolina 27706
1	ATTN: Information Processing Office
	Commanding General, U. S. Army Materiel Command, Washington, D. C. 20315
1	ATTN: AMCRD-RC-M
	Commanding General, Deseret Test Center, Fort Douglas, Utah 84113
1	ATTN: Technical Information Office
	Commanding General, U. S. Army Electronics Command, Fort Monmouth, New Jersey 07703
2	ATTN: AMSEL-RD-MAT
	Commanding General, U. S. Army Missile Command, Redstone Arsenal, Alabama 35809
1	ATTN: Technical Library
1	Mr. C. Martens
	Commanding General, U. S. Army Munitions Command, Dover, New Jersey 07801
1	ATTN: Technical Library

No. of Copies	To
	Commanding General, U. S. Army Satellite Communications Agency, Fort Monmouth, New Jersey 07703
1	ATTN: Technical Document Center
	Commanding General, U. S. Army Tank-Automotive Center, Warren, Michigan 48090
2	ATTN: SMOTA-RTS, Tech Data Coord Br
1	SMOTA-RCM.1
	Commanding General, U. S. Army Weapons Command, Research and Development Directorate, Rock Island, Illinois 61201
1	ATTN: AMSWE-RDR
	Commanding General, White Sands Missile Range, New Mexico 88002
1	ATTN: STEWS-WS-VT
	Commanding Officer, Aberdeen Proving Ground, Maryland 21005
1	ATTN: Technical Library, Building 313
	Commanding Officer, Edgewood Arsenal, Edgewood Arsenal, Maryland 21010
1	ATTN: Dir. of Eng. and Ind. Serv., Chem-Mun. Br. (Mr. F. E. Thompson)
	Commanding Officer, Frankford Arsenal, Bridge and Tacony Streets, Philadelphia, Pennsylvania 19137
1	ATTN: Library Branch C 2500
	Commanding Officer, Department of the Army, Ohio River Division Laboratories, Corps of Engineers, 5851 Mariemont Avenue, Cincinnati, Ohio 45227
1	ATTN: ORDLB-TR
	Commanding Officer, Picatinny Arsenal, Dover, New Jersey 07801
1	ATTN: SMUPA-VA6
	Commanding Officer, Redstone Scientific Information Center, U. S. Army Missile Command, Redstone Arsenal, Alabama 35809
4	ATTN: AMSMI-RBLD, Document Section
	Commanding Officer, Watervliet Arsenal, Watervliet, New York 12189
1	ATTN: SWEWV-RDT, Technical Information Services Office
1	Commanding Officer, U. S. Army Aviation Materiel Laboratories, Fort Eustis, Virginia 23604
	Commanding Officer, U. S. Army Aviation School Library, Fort Rucker, Alabama 36360
1	ATTN: USAAVNS-P&NRI

No. of Copies	To
	Commanding Officer, USACDC Ordnance Agency, Aberdeen Proving Ground, Maryland 21005
2	ATTN: Library, Building 305
	Director, Naval Research Laboratory, Anacostia Station, Washington, D. C. 20390
1	ATTN: Technical Information Officer
	Chief, Office of Naval Research, Department of the Navy, Washington, D. C. 20315
1	ATTN: Code 423
	Headquarters, Aeronautical Systems Division, Wright-Patterson Air Force Base, Ohio 45433
5	ATTN: ASRCEE
1	U. S. Atomic Energy Commission, Office of Technical Information Extension, P. O. Box 62, Oak Ridge, Tennessee 37830
	National Aeronautics and Space Administration, Washington, D. C. 20546
1	ATTN: Mr. B. G. Achhammer
1	Mr. G. C. Deutsch
1	Mr. R. V. Rhode
	National Aeronautics and Space Administration, Marshall Space Flight Center, Huntsville, Alabama 35812
1	ATTN: R-P&VE-M, Dr. W. R. Lucas
1	M-P&AE-M, Mr. W. A. Wilson, Building 4720
	Commanding Officer, U. S. Army Materials Research Agency, Watertown, Massachusetts 02172
5	ATTN: AMXMR-AT
1	AMXMR-AA
1	AMXMR-RP
1	AMXMR-RX
2	Authors
76	TOTAL COPIES DISTRIBUTED

UNCLASSIFIED
Security Classification

DOCUMENT CONTROL DATA - R&D

(Security classification of title, body of abstract and indexing annotation must be entered when the overall report is classified)

1. ORIGINATING ACTIVITY (Corporate author) U. S. Army Materials Research Agency Watertown, Massachusetts 02172	2a. REPORT SECURITY CLASSIFICATION Unclassified 2b. GROUP

3. REPORT TITLE
TEMPERED MARTENSITE EMBRITTLEMENT AND FRACTURE TOUGHNESS IN 4340 STEEL

4. DESCRIPTIVE NOTES (Type of report and inclusive dates)

5. AUTHOR(S) (Last name, first name, initial)
Kula, E. B., and
Anctil, A. A.

6. REPORT DATE	7a. TOTAL NO. OF PAGES	7b. NO. OF REFS
January 1967	21	45

8a. CONTRACT OR GRANT NO.	9a. ORIGINATOR'S REPORT NUMBER(S)
b. PROJECT NO. D/A 1C024401A328	AMRA TR 67-03
c. AMCMS Code 5025.11.294	9b. OTHER REPORT NO(S) (Any other numbers that may be assigned this report)
d. Subtask 35457	

10. AVAILABILITY/LIMITATION NOTICES
Distribution of this document is unlimited.

11. SUPPLEMENTARY NOTES	12. SPONSORING MILITARY ACTIVITY U. S. Army Materiel Command Washington, D. C. 20315

13. ABSTRACT

Tempered martensite embrittlement (500 F embrittlement) has been studied in 4340 steel by means of Charpy impact, tension, and fracture toughness tests carried out over a range of test temperatures. Embrittlement was shown in the impact tests by a minimum in room temperature impact properties for tempering temperatures ranging from 500 to 650 F, the same range for which the transition temperature is a maximum. No evidence of embrittlement was found in tension or room temperature fracture toughness tests. Embrittlement was noted, however, in fracture toughness tests carried out at -50 and -100 F, which indicates that low temperature testing will be necessary for proper materials evaluation. The plane strain fracture toughness (K_{Ic}) of various heats of 4340 steel has been correlated with the weight percent sulfur and phosphorus in the steel.

A mechanism for tempered martensite embrittlement is proposed. Certain impurity elements, such as phosphorus, which are more soluble in ferrite than in cementite, will segregate in the ferrite adjacent to the cementite shortly after the cementite precipitation. This transient enrichment of ferrite by impurity elements will be embrittling when the cementite is in a platelet or filmy form, and particularly so in the region of the prior austenite grain boundaries, where the impurity content may be higher than average. (Authors)

DD FORM 1 JAN 64 1473

UNCLASSIFIED
Security Classification

UNCLASSIFIED
Security Classification

KEY WORDS	LINK A		LINK B		LINK C	
	ROLE	WT	ROLE	WT	ROLE	WT
Steel (4340) Mechanical properties Fracture (toughness) Embrittlement Tensile properties Metals Temperature						

INSTRUCTIONS

1. ORIGINATING ACTIVITY: Enter the name and address of the contractor, subcontractor, grantee, Department of Defense activity or other organization *(corporate author)* issuing the report.

2a. REPORT SECURITY CLASSIFICATION: Enter the overall security classification of the report. Indicate whether "Restricted Data" is included. Marking is to be in accordance with appropriate security regulations.

2b. GROUP: Automatic downgrading is specified in DoD Directive 5200.10 and Armed Forces Industrial Manual. Enter the group number. Also, when applicable, show that optional markings have been used for Group 3 and Group 4 as authorized.

3. REPORT TITLE: Enter the complete report title in all capital letters. Titles in all cases should be unclassified. If a meaningful title cannot be selected without classification, show title classification in all capitals in parenthesis immediately following the title.

4. DESCRIPTIVE NOTES: If appropriate, enter the type of report, e.g., interim, progress, summary, annual, or final. Give the inclusive dates when a specific reporting period is covered.

5. AUTHOR(S): Enter the name(s) of author(s) as shown on or in the report. Enter last name, first name, middle initial. If military, show rank and branch of service. The name of the principal author is an absolute minimum requirement.

6. REPORT DATE: Enter the date of the report as day, month, year; or month, year. If more than one date appears on the report, use date of publication.

7a. TOTAL NUMBER OF PAGES: The total page count should follow normal pagination procedures, i.e., enter the number of pages containing information.

7b. NUMBER OF REFERENCES: Enter the total number of references cited in the report.

8a. CONTRACT OR GRANT NUMBER: If appropriate, enter the applicable number of the contract or grant under which the report was written.

8b, 8c, & 8d. PROJECT NUMBER: Enter the appropriate military department identification, such as project number, subproject number, system numbers, task number, etc.

9a. ORIGINATOR'S REPORT NUMBER(S): Enter the official report number by which the document will be identified and controlled by the originating activity. This number must be unique to this report.

9b. OTHER REPORT NUMBER(S): If the report has been assigned any other report numbers *(either by the originator or by the sponsor)*, also enter this number(s).

10. AVAILABILITY/LIMITATION NOTICES: Enter any limitations on further dissemination of the report, other than those imposed by security classification, using standard statements such as:

(1) "Qualified requesters may obtain copies of this report from DDC."

(2) "Foreign announcement and dissemination of this report by DDC is not authorized."

(3) "U. S. Government agencies may obtain copies of this report directly from DDC. Other qualified DDC users shall request through _____."

(4) "U. S. military agencies may obtain copies of this report directly from DDC. Other qualified users shall request through _____."

(5) "All distribution of this report is controlled. Qualified DDC users shall request through _____."

If the report has been furnished to the Office of Technical Services, Department of Commerce, for sale to the public, indicate this fact and enter the price, if known.

11. SUPPLEMENTARY NOTES: Use for additional explanatory notes.

12. SPONSORING MILITARY ACTIVITY: Enter the name of the departmental project office or laboratory sponsoring *(paying for)* the research and development. Include address.

13. ABSTRACT: Enter an abstract giving a brief and factual summary of the document indicative of the report, even though it may also appear elsewhere in the body of the technical report. If additional space is required, a continuation sheet shall be attached.

It is highly desirable that the abstract of classified reports be unclassified. Each paragraph of the abstract shall end with an indication of the military security classification of the information in the paragraph, represented as *(TS)*, *(S)*, *(C)*, or *(U)*.

There is no limitation on the length of the abstract. However, the suggested length is from 150 to 225 words.

14. KEY WORDS: Key words are technically meaningful terms or short phrases that characterize a report and may be used as index entries for cataloging the report. Key words must be selected so that no security classification is required. Identifiers, such as equipment model designation, trade name, military project code name, geographic location, may be used as key words but will be followed by an indication of technical context. The assignment of links, rules, and weights is optional.

UNCLASSIFIED
Security Classification